

Transition Curve with Smoothed Curvature at its Ends for Railway Roads

Wladyslaw Koc^{1*}

¹*Faculty of Civil and Environmental Engineering, Gdansk University of Technology, 11/12 G. Narutowicza Str., 80-233 Gdansk, Poland.*

Author's contribution

The sole author designed, analyzed and interpreted and prepared the manuscript.

Article Information

DOI: 10.9734/CJAST/2017/35006

Editor(s):

(1) Jakub Kostecki, Department of Civil and Environmental Engineering, University of Zielona Góra, Poland.

Reviewers:

(1) Abdullah Sonmezoglu, Bozok University, Turkey.

(2) Yong X. Gan, California State Polytechnic University, USA.

(3) Halil Görgün, Dicle University, Turkey.

Complete Peer review History: <http://www.sciencedomain.org/review-history/20057>

Original Research Article

Received 23rd June 2017

Accepted 12th July 2017

Published 15th July 2017

ABSTRACT

In the paper, in view of a railway ballasted track, a new concept of transition curve of linear form of curvature along its length and smoothed extreme regions is presented. For this purpose use has been made of an original, universal method for identifying transition curves by means of differential equations. Some general curvature equations for three regions investigated have been determined to be followed by appropriate parametric formulae. The possibility of determining the rectangular coordinates by numerical integration has been indicated. Taking into consideration the criterion of practical execution, and on account of very small horizontal ordinates in the initial region, a suggestion is made to reduce the length of the extreme regions and for such a case some particular theoretical relations have been worked out.

Keywords: Railway route; geometric layout; transition curve; curvature modeling.

1. INTRODUCTION

The transition curve issues related to vehicular roads and railway tracks are still under

investigation. The search for new forms of curves [1-13] is going on, including among others the dynamic model of the rail carriage – track system.

*Corresponding author: E-mail: kocwl@pg.gda.pl, wladyslaw.koc@pg.edu.pl;

Most of the transition curves are connected together by a common algorithm to determine the curvature using differential equations [14-16]. The curvature function $k(l)$ should be searched for among the differential equation

$$k^{(m)}(l) = f[l, k, k', k'', \dots, k^{(m-1)}] \quad (1)$$

with conditions

$$k^{(i)}(0^+) = 0 \quad \text{for } i = 1, 2, 3, \dots, n_1$$

$$k^{(j)}(l_k^-) = \begin{cases} \frac{1}{R} & \text{for } j = 0 \\ 0 & \text{for } j = 1, 2, 3, \dots, n_2 \end{cases} \quad (2)$$

Where

R – radius of the circular arc,
 l_k – length of the transition curve.

Making use of conditions (2) caused function $k(l)$ to be in class C^n within the interval $l \in \langle 0, l_k \rangle$ where $n = \min(n_1, n_2)$. Differential equation (1) could be a linear differential equation of constant or variable coefficients, homogeneous or nonhomogeneous. In most commonly applied solutions an equal number of conditions is assumed on both ends of the interval, i. e. $n_1 = n_2$. For two conditions, that is, $i = j = 0$ it is possible to obtain a linear curvature. With regard to a greater number of conditions the curvature along the whole length indicates a nonlinear form.

The presented way of proceeding leads, in principle, to the acquisition of nonlinear curvature along the transition curve length. Only in one case, for $n_1 = n_2$, one can obtain the linear curvature. And such a solution has been commonly used for a number of years in vehicular, railway and water-way traffic. The transition curve which corresponds to it is a clothoid. However on railway roads use is made of its simplified form known as third degree parabola (although at present taking into consideration the calculation capabilities it has no justification).

At this point it is necessary to note that the curvature of the transition curve determines also the shape of the gradient due to cant. The linear curvature along its length indicates a necessity to apply a linear gradient due to cant. But, for the

reason that the exploitation of the railway track causes its vertical deformations, the damaged shape of the gradient due to cant should constantly be restored and it is undoubtedly easier to do by some attempts at linear exploitation. Therefore such a solution that has commonly been applied for a long time, should not cause any astonishments. For many years a superstructure using a broken stone has become a standard railway track construction requiring, in principle, a constant execution of maintenance works.

The major drawback of the clothoid (of linear curvature) is the occurrence of bends on the diagram of its curvature in the initial and end regions. This is adverse from the view point of the dynamic interactions in the rail carriage – track system. An improvement of the situation should therefore be based on smoothing the curvature in these regions. Meanwhile an alternative to the linear curvature are the solutions relating to its nonlinear form along the entire length of the transition curve. And this fact, in exploitation of broken stone superstructure, can cause adversion to practical use of smooth transition curves which are known for a very long time. The occurrence of the nonlinear curvature along the transition curve indicates a necessity to apply a nonlinear gradient due to cant.

This situation is subject to a radical change in consequence of a wide use of ballastless track, e. g. the use of concrete plate. This occurs mainly on high speed railways. The vertical deformations that can be found in such a superstructure are relatively small and can easily be eliminated. For this reason smooth transition curves are fully applied here.

However, if in a given country the classic superstructure is still used on crushed-stone bed, the linear curvature is furtheron preferable. For instance, in France and in the USA in order to improve the existing disadvantageous situation the extreme regions of the transition curves in clothoidal form are modified for the purpose of eliminating bends on the curvature diagram and obtaining its nonlinear performance. French railway systems take advantage of such solutions not only with regard to high speed railway lines, but also in conventional systems where speeds exceed 100 kph [17]. It is also worthy of mention that the benefits resulting from the linear proceeding of the curvature (and the linear gradients due to cant) are indicated also by some model testes of the rail carriage – track system.



Of course the bends found on both sides of the curvature diagram (by making use of linear curvature) correspond to the two bends of the gradient due to cant. And, just the two bends are responsible for the fundamental realizability problem. The realizability practice univocally proves that just in these regions the accuracy of the tamping machine leaves much to be expected. In paper [18] an attempt has been made to smooth out only the regions of the gradient due to cant itself. This indicated an intentional departure from principles relating to the modeling of the transition curve formation and the gradient due to cant and caused certain disturbances in the system of the occurring unbalanced accelerations. However, the effects of the disturbances were certainly minor than the real ones, resulting from incorrect operation of the tamping machine.

Under conditions of this situation it seems purposeful to elaborate the theoretical fundamentals for a new transition curve of a linear form of curvature along its length and smoothed out extreme regions. For this purpose use will be made a universal method of identifying the transition curves by means of differential equations [15,16,19].

2. DETERMINATION OF GENERAL CURVATURE EQUATIONS

After the adoption of coefficient $C \leq 0.25$ the transition curve of length l_k is divided into three zones (Fig. 1):

- initial region of length $C \cdot l_k$ provided with a smooth curvature diagram,

- mid-region of length $(1 - 2C)l_k$ provided with linear curvature,
- final region of length $C \cdot l_k$ provided with smooth curvature.

At the outset of the transition curve, curvature $k(0) = 0$, whereas at its end $k(l_k) = \frac{1}{R}$.

As it follows from Fig. 1, the mid-region ($l \in \langle Cl_k, l_k - Cl_k \rangle$) of linear characteristic of the the curvature should have a slope coefficient bigger than the mean value along the entire length of the transition curve. Thus it is assumed that $k'(l) = \frac{D}{Rl_k}$, where $D > 1$ (precise boundaries

for this parameter will be determined using the solution analysis for the curve initial region). Due to such an assumption it is possible to find the curvature values at the beginning and end of the mid-region.

2.1 Initial Region $l \in \langle 0, Cl_k \rangle$

The following boundary conditions and the differential equation (for polynomial solution) are assumed:

$$\left\{ \begin{array}{l} k(0) = 0, \quad k(Cl_k) = \frac{1 - D(1 - 2C)}{2R}, \\ k'(0) = 0, \quad k'(Cl_k) = \frac{D}{Rl_k} \end{array} \right. \quad (3)$$

$$k^{(4)}(l) = 0 \quad (4)$$

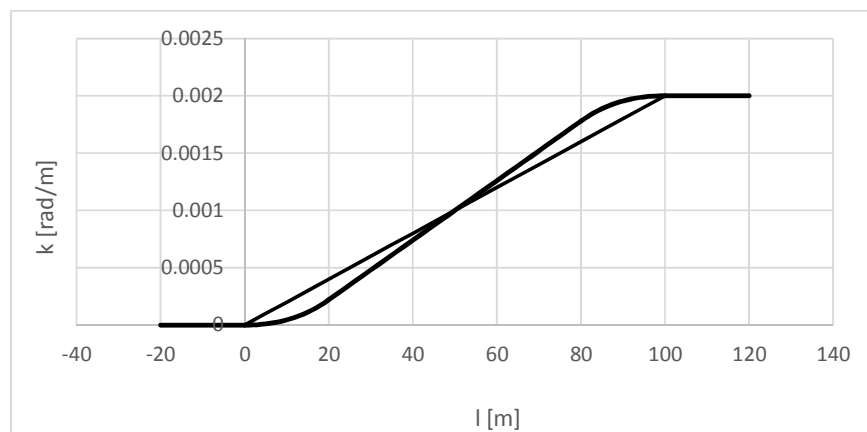


Fig. 1. Schematic diagram of solving the problem (for $R = 500$ m and $l_k = 100$ m)

In consequence of solving the differential problem (3), (4) the following curvature equation is obtained:

$$k(l) = a_{11}l^2 + a_{12}l^3 \quad (5)$$

Where

$$a_{11} = \frac{3-3D(1-C)+CD}{2C^2Rl_k^2}, \quad a_{12} = -\frac{1-D(1-C)}{C^3Rl_k^3}.$$

The correct solution makes it necessary to select appropriate set of parameters C and D . For the adopted C it is not sufficient to satisfy condition $D > 1$. Curvature function $k(l)$ must be a monotonic one rising for $l > 0$; hence the condition

$$k'(l) = \left[\frac{3-3D(1-C)+CD}{C^2Rl_k^2} - \frac{3-3D(1-C)}{C^3Rl_k^3} \right] l \geq 0 \quad (6)$$

By here may be no inflexion points, and the required convexity down sets another condition

$$k''(l) = \frac{3-3D(1-C)+CD}{C^2Rl_k^2} - \frac{6-6D(1-C)}{C^3Rl_k^3} l \geq 0 \quad (7)$$

Condition (6) indicates that

$$\frac{3-3D(1-C)+CD}{C^2Rl_k^2} - \frac{3-3D(1-C)}{C^3Rl_k^3} l \geq 0$$

The boundary of the area is given by a straight line, while the adopted condition should be fulfilled on both its ends. The transformation and

the use of the random variable $\xi = \frac{l}{l_k}$ provides

$$3C - 3CD + 4C^2D - 3(1-D+CD)\xi \geq 0, \quad \xi \in \langle 0, C \rangle$$

At the initial point for $\xi = 0$, $3C - 3CD + 4C^2D \geq 0$, hence

$$D \leq \frac{3}{3-4C} \quad (8)$$

At the end of the interval, for $\xi = C$, $3C - 3CD + 4C^2D - 3(1-D+CD)C \geq 0$, hence it follows that $C^2D \geq 0$, where the condition is always satisfied.

From Equation (7) it also follows that the boundary of the region is marked by a straight; after transformation and application of random variable ξ

$$3C - 3CD + 4C^2D - 6(1-D+CD)\xi \geq 0, \quad \xi \in \langle 0, C \rangle$$

For $\xi = 0$ condition (8) is obtain again, while for $\xi = C$

$$3C - 3CD + 4C^2D - 6(1-D+CD)C \geq 0,$$

hence

$$D \geq \frac{3}{3-2C} \quad (9)$$

Conditions (8) and (9) provide an interval of parameter values D .

$$\frac{3}{3-2C} \leq C \leq \frac{3}{3-4C} \quad (10)$$

The boundary values of parameter D have been presented in Table 1.

2.2 Middle Region $l \in \langle Cl_k, l_k - Cl_k \rangle$

The middle section is bound by conditions

$$k(Cl_k) = \frac{1-D(1-2C)}{2R}, \quad k(l_k - Cl_k) = \frac{1+D(1-2C)}{2R} \quad (11)$$

and the differential equation

$$k''(l) = 0 \quad (12)$$

This provides the linear curvature equation

$$k(l) = a_{21} + a_{22}l \quad (13)$$

where $a_{21} = \frac{1-C}{2R}$, $a_{22} = \frac{D}{Rl_k}$.

2.3 Final Region $l \in \langle l_k - Cl_k, l_k \rangle$

The final segment is encumbered with differential equation (4) and the following boundary conditions

$$\left\{ \begin{array}{l} k(l_k - Cl_k) = \frac{1 + D(1 - 2C)}{2R}, \quad k(l_k) = \frac{1}{R}, \\ k'(l_k - Cl_k) = \frac{D}{Rl_k}, \quad k'(l_k) = 0. \end{array} \right. \quad (14)$$

$$x(l) = \int \cos \Theta(l) dl \quad (16)$$

$$y(l) = \int \sin \Theta(l) dl \quad (17)$$

$$\Theta(l) = \int k(l) dl \quad (18)$$

The curvature function is described by

$$k(l) = a_{31} + a_{32}l + a_{33}l^2 + a_{34}l^3 \quad (15)$$

where

$$a_{31} = \frac{2 - 3C + 2C^3 + 5CD - 4C^2D - 2D}{2C^3R},$$

$$a_{32} = -\frac{3 - 3C + 6CD - 4C^2D - 3D}{C^3Rl_k},$$

$$a_{33} = \frac{6 - 3C + 9CD - 4C^2D - 6D}{2C^3Rl_k^2},$$

$$a_{34} = -\frac{1 + CD - D}{C^3Rl_k^3}.$$

Fig. 2 gives an example of solution of the problem relating to the following data: $R = 500$ m, $l_k = 100$ m, $C = 0.2$ and $D = 1.3$.

3. DETERMINATION OF PARAMETRIC EQUATIONS

The parametric equations of the smoothed transition curve are determined using the following formulae:

An analytical solution of the problem requires an expansion of semi-differential functions $\cos \Theta(l)$ and $\sin \Theta(l)$ into a Taylor (or Maclaurin) series and an integration of individual expressions. To expand the function into a series use has been made of the Maxima programme [20]. Further part of the paper gives a comparison of parametric equations obtained for particular regions of the transition curve (not involving any insignificant expressions).

3.1 Initial Region $l \in \langle 0, Cl_k \rangle$

$$\Theta(l) = A_{11}l^3 + A_{12}l^4 \quad (19)$$

where

$$A_{11} = \frac{a_{11}}{3} = \frac{3 - 3D(1 - C) + CD}{6C^2Rl_k^2}, \quad A_{12} = \frac{a_{12}}{4} = -\frac{1 - D(1 - C)}{4C^3Rl_k^3}$$

The parametric equations are as follows:

$$x(l) = l \quad (20)$$

$$y(l) = \frac{A_{11}}{4}l^4 + \frac{A_{12}}{5}l^5 \quad (21)$$

Table 1. Boundary values of parameter D for various characteristics of C

| C | D_{min} | D_{max} | C | D_{min} | D_{max} |
|------|-----------|-----------|------|-----------|-----------|
| 0 | 1 | 1 | 0.13 | 1.09489 | 1.20968 |
| 0.01 | 1.00671 | 1.01351 | 0.14 | 1.10294 | 1.22951 |
| 0.02 | 1.01351 | 1.02740 | 0.15 | 1.11111 | 1.25000 |
| 0.03 | 1.02041 | 1.04167 | 0.16 | 1.11940 | 1.27119 |
| 0.04 | 1.02740 | 1.05634 | 0.17 | 1.12782 | 1.29310 |
| 0.05 | 1.03448 | 1.07143 | 0.18 | 1.13636 | 1.31579 |
| 0.06 | 1.04167 | 1.08696 | 0.19 | 1.14504 | 1.33929 |
| 0.07 | 1.04895 | 1.10294 | 0.20 | 1.15385 | 1.36364 |
| 0.08 | 1.05634 | 1.11940 | 0.21 | 1.16279 | 1.38889 |
| 0.09 | 1.06383 | 1.13636 | 0.22 | 1.17187 | 1.41509 |
| 0.10 | 1.07143 | 1.15385 | 0.23 | 1.18110 | 1.44231 |
| 0.11 | 1.07914 | 1.17187 | 0.24 | 1.19048 | 1.47059 |
| 0.12 | 1.08696 | 1.19048 | 0.25 | 1.20000 | 1.50000 |



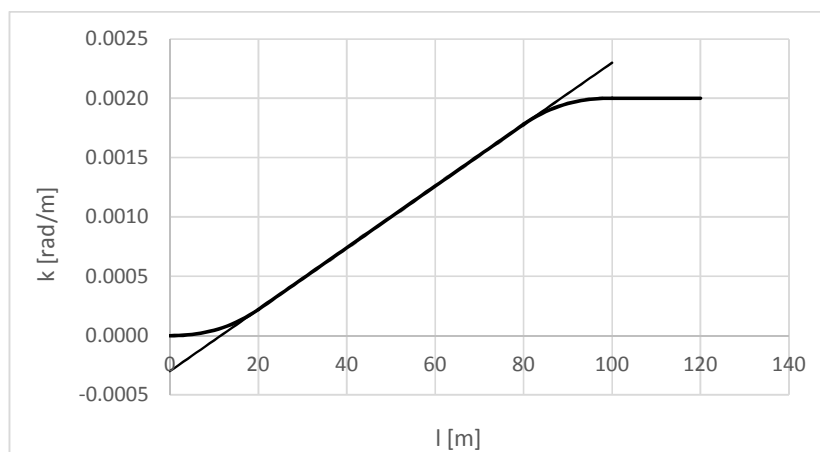


Fig. 2. Diagram of curvature smoothed for $R = 500$ m, $l_k = 100$ m, $C = 0.2$ and $D = 1.3$

3.2 Middle Region $l \in \langle Cl_k, l_k - Cl_k \rangle$

$$\Theta(l) = A_{21} + A_{22}l + A_{23}l^2 \quad (22)$$

Where

$$A_{21} = \frac{3D - CD - 3}{12R} Cl_k, \quad A_{22} = a_{21} = \frac{1 - D}{2R}, \quad A_{23} = \frac{a_{22}}{2} = \frac{D}{2Rl_k}.$$

The coordinates for this region are described by the following parametric equations:

$$x(l) = x_1(Cl_k) + \cos A_{20}(l - l_{20}) - \frac{1}{2}(A_{22} + 2A_{23}l_0) \sin A_{20}(l - l_{20})^2 - \frac{1}{6}[(A_{22}^2 + 4A_{22}A_{23}l_0 + 4A_{23}^2l_0^2) \cos A_{20} + 2A_{23} \sin A_{20}](l - l_{20})^3 - \frac{1}{4}(2A_{23}^2l_{20} + A_{22}A_{23}) \cos A_{20}(l - l_{20})^4 - \frac{1}{10}A_{23}^2 \cos A_{20}(l - l_{20})^5 \quad (23)$$

$$y(l) = y_1(Cl_k) + \sin A_{20}(l - l_{20}) + \frac{1}{2}(A_{22} + 2A_{23}l_{20}) \cos A_{20}(l - l_{20})^2 - \frac{1}{6}[(A_{22}^2 + 4A_{22}A_{23}l_0 + 4A_{23}^2l_0^2) \sin A_{20} - 2A_{23} \cos A_{20}](l - l_{20})^3 \quad (24)$$

Where

$$x_1(Cl_k), \quad y_1(Cl_k) \quad - \quad \text{from the initial region}$$

$$l_{20} = Cl_k, \quad A_{20} = A_{21} + A_{22}l_{20} + A_{23}l_{20}^2.$$

3.3 Final Region $l \in \langle l_k - Cl_k, l_k \rangle$

$$\Theta(l) = A_{31} + A_{32}l + A_{33}l^2 + A_{34}l^3 + A_{35}l^4 \quad (25)$$

where

$$A_{31} = -\frac{3 - 6C + 6C^3 + 9CD - 8C^2D - 3D}{12C^3R}, \quad A_{32} = a_{31} = \frac{2 - 3C + 2C^3 + 5CD - 4C^2D - 2D}{2C^3R}$$

$$A_{33} = \frac{a_{32}}{2} = -\frac{3 - 3C + 6CD - 4C^2D - 3D}{2C^3Rl_k}, \quad A_{34} = \frac{a_{33}}{3} = \frac{6 - 3C + 9CD - 4C^2D - 6D}{6C^3Rl_k^2},$$

$$A_{35} = \frac{a_{34}}{4} = -\frac{1 + CD - D}{4C^3Rl_k^3}.$$

Parametric equations $x(l)$ and $y(l)$ are:

$$x(l) = x_2[(1 - C)l_k] + \cos A_{30}(l - l_{30}) - \frac{1}{2}[(2 A_{33}l_{30} + 3 A_{34}l_{30}^2 + 4 A_{35}l_{30}^3 + A_{32}) \sin A_{30}](l - l_{30})^2 - \frac{1}{6}[(4 A_{33}^2l_{30}^2 + 12 A_{33} A_{34}l_{30}^3 + 16 A_{33} A_{35}l_{30}^4 + 9 A_{34}^2l_{30}^4 + 24 A_{34} A_{35}l_{30}^5 + 16 A_{35}^2l_{30}^6 + 8 A_{32} A_{35}l_{30}^3 + 6 A_{32} A_{34}l_{30}^2 + 4 A_{32} A_{33}l_{30} + A_{32}^2) \cos A_{30} + (2 A_{33} + 6 A_{34}l_{30} + 12 A_{35}l_{30}^2) \sin A_{30}](l - l_{30})^3 \quad (26)$$

$$y(l) = y_2[(1 - C)l_k] + \sin A_{30}(l - l_{30}) + \frac{1}{2}[(2 A_{33}l_{30} + 3 A_{34}l_{30}^2 + 4 A_{35}l_{30}^3 + A_{32}) \cos A_{30}](l - l_{30})^2 - \frac{1}{6}[(4 A_{33}^2l_{30}^2 + 12 A_{33} A_{34}l_{30}^3 + 16 A_{33} A_{35}l_{30}^4 + 9 A_{34}^2l_{30}^4 + 24 A_{34} A_{35}l_{30}^5 + 16 A_{35}^2l_{30}^6 + 8 A_{32} A_{35}l_{30}^3 + 6 A_{32} A_{34}l_{30}^2 + 4 A_{32} A_{33}l_{30} + A_{32}^2) \sin A_{30} - (2 A_{33} + 6 A_{34}l_{30} + 12 A_{35}l_{30}^2) \cos A_{30}](l - l_{30})^3 \quad (27)$$

where

$$x_2[(1 - C)l_k], \quad y_2[(1 - C)l_k] \quad - \text{from the middle region}$$

$$l_{30} = (1 - C)l_k, \quad A_{30} = A_{31} + A_{32}l_{30} + A_{33}l_{30}^2 + A_{34}l_{30}^3 + A_{35}l_{30}^4$$

4. NUMERIC INTEGRATION METHOD

The analytical form of equations for horizontal coordinates, especially in the middle and final regions, is quite complex, which does not comply with the users expectations. This can be indicated, among others, in commercial computer design aided programmes for track geometric layouts [21,22]. The Cartesian coordinates are obtained here by numerical integration. For this purpose it is necessary to adopt an adequate calculation step d , and to divide the transition curve into $n = \frac{l_k}{d}$ intervals. Other coordinates are determined by the use of the following formulae:

$$x(l_p) = \frac{1}{2}d \sum_{i=1}^p |\cos \theta(l_i) - \cos \theta(l_{i-1})| \quad (28)$$

$$y(l_p) = \frac{1}{2}d \sum_{i=1}^p |\sin \theta(l_i) - \sin \theta(l_{i-1})| \quad (29)$$

where $p = 1, 2, \dots, n$.

The numerical procedure has been proved in numerous cases by taking advantage of calculation step 0.5 m and 1 m. Following this

procedure it was possible to obtain a complete conformity with the results of the analytical technique. Undoubtedly this is connected with the regular form of function $\theta(l)$. However, it does not mean to avoid using the analytical method which has a universal character and creates additional interpreting capabilities.

5. PREFERABLE FORM OF CURVE

When applying the transition curve one should take into consideration the occurrence of very small horizontal ordinates in the initial region. Very often they are hard to execute and in practice it causes elongation of the track straight segment. Therefore the lengths of extreme regions should be limited. By adopting this procedure the length of the mid-region becomes bigger and assumes a linear form of the curvature. An assumption has been made that the value of factor C for the preferred form of curve will reach $C = 0.05$, and coefficient D (using table 1) – $D = 1.06$. In this way it is possible to obtain equations for curvature and the adequate parametric formulae for some specific transition curve regions.



5.1 Initial Region $l \in \langle 0; 0.05l_k \rangle$

$$y(l) = \frac{8}{15Rl_k^2}l^4 + \frac{14}{5Rl_k^3}l^5 \quad (32)$$

$$k(l) = \frac{32}{5Rl_k^2}l^2 + \frac{56}{Rl_k^3}l^3 \quad (30)$$

$$x(l) = l \quad (31)$$

5.2 Middle Region $l \in \langle 0.05l_k; 0.95l_k \rangle$

$$k(l) = -\frac{3}{100R} + \frac{53}{50Rl_k}l \quad (33)$$

$$x(l) = x_1(0,05 l_k) + \cos A_{20}(l - 0,05 l_k) + \frac{1}{24} \left[\left(-\frac{7314}{R^2 l_k} 10^{-5} \right) \cos A_{20} + \left(\frac{12167}{R^2} 10^{-9} \right) \sin A_{20} \right] (l - 0,05 l_k)^4 + \frac{1}{120} \left[\left(\frac{33708}{R^2 l_k^2} 10^{-4} + \frac{279841}{R^4} 10^{-12} \right) \cos A_{20} + \left(\frac{336444}{R^2 l_k} 10^{-8} \right) \sin A_{20} \right] (l - 0,05 l_k)^5 \quad (34)$$

$$y(l) = y_1(0,05 l_k) + \sin A_{20} (l - 0,05 l_k) + \left(\frac{23}{2R} 10^{-3} \right) \cos A_{20} (l - 0,05 l_k)^2 - \frac{1}{6} \left[\left(-\frac{106}{R l_k} 10^{-2} \right) \cos A_{20} + \left(\frac{529}{R^2} 10^{-6} \right) \sin A_{20} \right] (l - 0,05 l_k)^3 \quad (35)$$

where $A_{20} = \frac{17}{48R} 10^{-3} l_k$.

5.3 Final Region $l \in \langle 0.95l_k; l_k \rangle$

$$k(l) = -\frac{307}{5R} + \frac{904}{5Rl_k}l - \frac{872}{5Rl_k^2}l^2 + \frac{56}{Rl_k^3}l^3 \quad (36)$$

$$x(l) = x_2(0,95 l_k) + \cos A_{30} (l - 0,95 l_k) - \left(\frac{977}{2R} 10^{-3} \right) \sin A_{30} (l - 0,95 l_k)^2 \quad (37)$$

$$y(l) = y_2(0,95 l_k) + \sin A_{30} (l - 0,95 l_k) + \left(\frac{977}{2R} 10^{-3} \right) \cos A_{30} (l - 0,95 l_k)^2 \quad (38)$$

where $A_{30} = \frac{13510625}{3R} 10^{-7} l_k$.

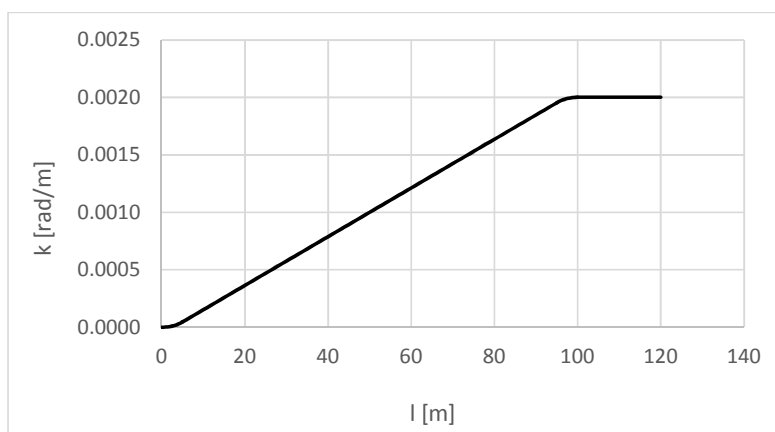


Fig. 3. Diagram of smoothed curvature for $R = 500$ m, $l_k = 100$ m, $C = 0.05$ and $D = 1.06$

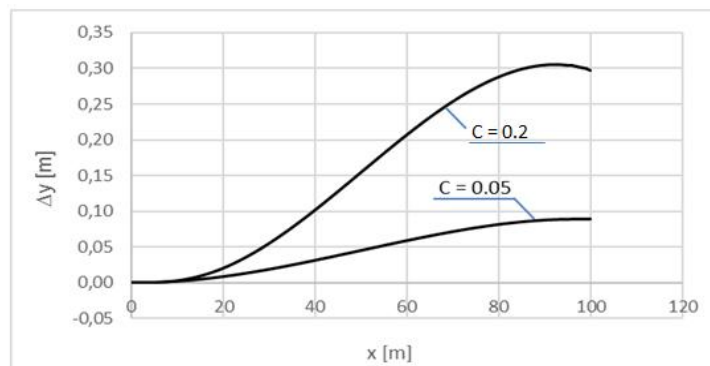


Fig. 4. Diagrams of ordinate variations for transition curves with smoothed curvature $C = 0.2$, $D = 1.3$ and $C = 0.05$, $D = 1.06$ with regard to clothoid ($R = 500$ m, $l_k = 100$ m)

Fig. 3 illustrates the curvature diagram for the following data: $R = 500$ m, $l_k = 100$ m, $C = 0.05$ and $D = 1.06$ while Fig. 4 provides schemes of variations of ordinates $\Delta y(l)$ for transition curves of Figs 2 and 3 with regard to clothoid described by parametric equations:

$$x(l) = l - \frac{1}{40 R^2 l_k^2} l^5 + \frac{1}{3456 R^4 l_k^4} l^9 - \frac{1}{599040 R^6 l_k^6} l^{13} + \dots \quad (39)$$

$$y(l) = \frac{1}{6 R l_k} l^3 - \frac{1}{336 R^3 l_k^3} l^7 + \frac{1}{42240 R^5 l_k^5} l^{11} - \dots \quad (40)$$

As can be seen the transition curve ordinates with smoothed curvature along their total length, are smaller than the clothoid ordinates. From Fig. 4 it follows that the differences are not big, in particular in the case of curve $C = 0.05$. This indicates that the indispensable cross-wise shift of the circular arc should not cause any significant location problems. An improvement of the situation, i. e. replacement of the clothoid by transition curve provided with smoothed curvature can be carried out in compliance with the standard regulation of the track axis.

6. CONCLUSIONS

The basic failure of the transition curve in the form of clothoid provided with linear curvature, is the appearance of bends in the diagram of its curvature in initial and end regions. This is a disadvantage from the viewpoint of dynamic interactions in the rail carriage – track system. An improvement of the situation should therefore be based on smoothing the curvature just in these regions. At the same time it will be advantageous to retain the linear character of the curvature in the remaining part of the curve for the reason that the straight gradient due to cant situated right there is relatively easy for current maintenance.

The problem is of particular significance when classic surface is still used in a country, where broken stone bed is used, and linear curvature is preferable. However, such a situation is subject to radical changes connected with the use of ballastless construction of the track, for instance, on a concrete plate. This procedure is mainly noted in areas of high speed railway systems. The vertical deformations that occur in such surfaces are relatively small and can be eliminated with ease. For this reason a full range of smooth transition curves finds application here, where the curvature along the whole length is nonlinear.

In the paper, in view of a track provided with broken-stone bed, a new concept of transition curve of linear form of curvature along its length and smoothed extreme regions is presented. For this purpose use has been made of an original, universal method for identifying transition curves by means of differential equations. Some general curvature equations for three regions investigated have been determined to be followed by appropriate parametric formulae. The possibility of determining the rectangular coordinates by numerical integration has been indicated. Taking into consideration the criterion of practical execution, and on account of very small horizontal ordinates in the initial region, a suggestion is made to reduce the length of the extreme regions and for such a case some particular theoretical relations have been worked out.

The application of the analyzed transition curve can become an alternative to smooth transition curves. It is possible to note a certain aversion in relations to their practical implementation. As can be expected this is presumably connected with the nonlinear gradient due to cant which occurs



on the curves. Under practical exploitation it is vertically deformed and its shape should constantly be renovated; undoubtedly it is easier to do this by making attempts to maintain the linear procedure.

COMPETING INTERESTS

Author has declared that no competing interests exist.

REFERENCES

1. Arslan A, Tari E, Ziatdinov R, Nabiyev R. Transition curve modeling with kinematical properties: Research on log-aesthetic curves. *Computer-Aided Design and Applications*. 2014;11(5):509-517.
2. Baykal O, Tari E, Coskun Z, Sahin M. New transition curve joining two straight lines. *Journal of Transportation Engineering, ASCE*. 1997;123(5):337-345.
3. Bosurgi G, D'andrea A. A polynomial parametric curve (PPC-CURVE) for the design of horizontal geometry of highways. *Computer-Aided Civil and Infrastructure Engineering*. 2012;27(4):303-312.
4. Cai H, Wang G. A new method in highway route design: Joining circular arcs by a single C-bezier curve with shape parameter. *Journal of Zhejiang University Science A*. 2009;10(4):562-569.
5. Habib Z, Sakai M. G^2 pythagorean hodograph quintic transition between two circles with shape control. *Computer Aided Geometric Design*. 2007;24:252-266.
6. Habib Z, Sakai M. On PH quantic spirals joining two circles with one circle inside the other. *Computer-Aided Design*. 2007;39: 125-132.
7. Kobryn A. New solutions for general transition curves. *Journal of Surveying Engineering, ASCE*. 2014;140(1):12-21.
8. Tari E, Baykal O. An alternative curve in the use of high speed transportation systems. *ARI*. 1998;51(2):126-135.
9. Tari E, Baykal O. A new transition curve with enhanced properties. *Canadian Journal of Civil Engineering*. 2011; 32(5):913-923.
10. Tasci I, Kuloglu N. Investigation of a new transition curve. *The Baltic Journal of Road and Bridge Engineering*. 2011;6(1):23-29.
11. Zboinski K, Woznica P. Optimization of the railway transition curves' shape with use of vehicle-track dynamical model. *Archives of Transport*. 2010;22(3):387-407.
12. Zboinski K, Woznica P. Formation of polynomial railway transition curves of even degrees. *Prace Naukowe Politechniki Warszawskiej, Transport*. 2014;101:189-202.
13. Ziatdinov R. 2012. Family of superspirals with completely monotonic curvature given in terms of Gauss hypergeometric function. *Computer Aided Geometric Design*. 2012;29(7):510-518.
14. Koc W. Theoretical elements of designing track layouts (in Polish). Gdansk: Gdansk University of Technology Publishing; 2004.
15. Koc W. Identification of transition curves in vehicular roads and railways. *Logistics and Transport*. 2015;28(4):31-42.
16. Mieloszyk E, Koc W. General dynamic method for determining transition curve equations. *Rail International-Schienen der Welt*. 1991;22(10):32-40.
17. Technical memorandum 2.1.2 – Alignment design standards for high-speed train operation. The California High-Speed Rail Authority; 2009.
18. Koc W. An attempt at smoothing the bends on a gradient due to cant (in Polish). *Sci.-Tech. Papers Association of Engineers and Technicians of the Republic of Poland, Cracow Division, series: Conference Papers*. 2011;96(158):197-209.
19. Koc W. Analytical method of modelling the geometric system of communication route. *Mathematical Problems in Engineering*. 2014;2014:Article ID 679817:13
20. Maxima, a computer algebra system. Available:<http://maksima.sourceforge.net>
21. AutoCAD Civil 3D. Autodesk. Available:<http://www.autodesk.pl>
22. Micro Station. Bentley Systems. Available:<http://www.bentley.com>

© 2017 Koc; This is an Open Access article distributed under the terms of the Creative Commons Attribution License (<http://creativecommons.org/licenses/by/4.0>), which permits unrestricted use, distribution, and reproduction in any medium, provided the original work is properly cited.

Peer-review history:
 The peer review history for this paper can be accessed here:
<http://sciencedomain.org/review-history/20057>